 doi:10.20944/preprints202102.0078.v1

Article

Inactivation of Human Coronavirus by Fathhome's Dry Sanitizer Device: Rapid and Eco-friendly Ozone-based disinfection of SARS-CoV-2

Timsy Uppal [1], Amir Khazaieli [2], Antoine M. Snijders [3] and Subhash C. Verma [1,*]

[1] Department of Microbiology and Immunology, University of Nevada, Reno School of Medicine, 1664 N Virginia Street, Reno, NV 89557; scverma@med.unr.edu
[2] FATHHOME, INC. 8000 Edgewater Drive Suite #200, Oakland, CA 94621
[3] Biological Systems and Engineering Division, Lawrence Berkeley National Laboratory, 1 Cyclotron Road, Berkeley, CA 94720
* Correspondence: scverma@med.unr.edu; Tel.: 775-682-6743 (S.C.V.)

Abstract: The pandemic history of pathogenic SARS-CoV-2 associated COVID-19 infection began in December 2019, with its emergence in Wuhan, China. Pertaining to its high transmissibility and wide host adaptability, this new and unique human coronavirus spread across the planet affecting almost every country, inflicting 91 million people and causing 1.9 million deaths (as of January 17th, 2021). Limited or negligible pre-existing immunity to multiple SARS-CoV-2 variants has resulted in severe morbidity and mortality worldwide, as well as a record-breaking surge in the use of medical-surgical supplies and personal protective equipments. In response to the global need for effective sterilization techniques, this study evaluated the virucidal efficacy of FATHHOME's self-contained, ozone-based dry-sanitizing device, by dose and time response assessment. We tested inactivation of human coronavirus, HCoV-OC43, a close genetic model of SARS-CoV-2, on porous (N95 filtering facepiece respirator/FFR) and nonporous (glass) surfaces. We started our assays with 20 ppm of ozone for 10 min exposure, which was able to effectively reduce, 99.8% and 99.9% of virus from glass and N95 FFR surfaces, respectively. Importantly, the virus was completely inactivated, below the detection limit (over 6-$\log_{10}$ reduction) with 25 ppm ozone for 15 mins on both tested surfaces. As expected, a higher ozone concentration (50 ppm) resulted in faster inactivation of HCoV-OC43 with 100% inactivation in 10 mins from both the surfaces, with no residual ozone present after completion of the 5-minute post exposure recapture cycle and no measurable increase in ambient ozone levels. These results confirmed that FATHHOME's device may provide a safe and viable solution for rapid decontamination of SARS-CoV-2- from worn items, frequently touched items, and PPE including N95 FFRs, face shields and other personal items.

Keywords: FATHHOME, SARS-CoV-2; COVID-19; Virus decontamination, PPEs

1. Introduction

The recently identified SARS-CoV-2, a *betacoronavirus* of zoonotic origin [1], has been implicated as the etiologic agent of the COVID-19 pandemic [2]. COVID-19 is a severe and potentially fatal infectious disease that can be spread by asymptomatic, presymptomatic and symptomatic carriers [3,4]. As of January 17th 2021, over 95.6 million people worldwide [5] have been infected with SARS-CoV-2, threatening human health and public safety. Even though a large portion of COVID-19 patients remain asymptomatic or mildly symptomatic, the infection causes serious complications in susceptible individuals [6]. COVID-19 disease is characterized by complications including endothelial barrier disruption, dysfunctional alveolar-capillary oxygen transmission, and impaired oxygen diffusion capacity [7]. In critical symptomatic cases, life threatening acute respiratory distress syndrome (ARDS) associated with hypoxaemic respiratory failure and non-cardiogenic pulmonary edema is the main cause of death [8–10]. SARS-CoV-2 mediated endothelial tissue injury is believed

 doi:10.20944/preprints202102.0078.v1

to cause alveolar permeability disruption and pulmonary vascular thrombosis in COVID-19 patients with ARDS [11].

Infections associated with the 2019 SARS-CoV-2 outbreak spread by contact, respiratory droplet, and airborne transmission [12]. Surfaces of animate and inanimate objects have been reported to contribute in the spread of SARS-CoV-2 infections [13,14]. The presence, stability, and infectivity potential of SARS-CoV-2 has been reported for different types of clinical samples (urine, sputum, blood, feces, and bronchoalveolar fluid) [15,16], on different surfaces (floor, door handle, bed rail, bedside table, microwave oven/closet/faucet handle, mobile phone, eyeglasses) [17,18], and on a variety of surface materials (metal, rubber, ceramic, surgical glove, wood, cloth, plastic, stainless steel, surgical mask, and tissue paper) [13]. SARS-CoV-2 is viable on inanimate surfaces, one of the most prone sites for the virus transmission, for prolonged times estimated to be between 2 hrs and 9 days, with virus persistence depending on the temperature, pH, relative humidity, and nature of the surface [19]. Although, vaccinations and anti-viral therapies are given the top priority to reduce the spread of COVID-19 disease, according to WHO guidelines, effective infection prevention and control (IPC) is a practical, evidence-based approach to restrict disease spread [12].

Current interventions for COVID-19 prevention include an effective surface disinfectant, appropriate hand hygiene, and personal protective equipment (PPE), primarily suitable face mask/respirator, gloves, face shield and gowns. According to United States Environmental Protection Agency (USEPA), effective surface disinfectants with significant virucidal activity at low contact time, mostly contain hydrogen peroxide, peroxyacetic acid, 70% ethanol, phenol, quaternary ammonium salt derivatives, aldehyde, hypochlorous acid, sodium hypochlorite, sodium bicarbonate, octanoic acid, citric acid, conjugates with silver ions, as the key active ingredients [12,20]. Kampf and Colleagues recently analysed 22 research reports that studied inactivation of SARS and MERS (human coronaviruses/HCoVs of epidemic potential) with biocidal agents, and revealed that surface disinfection using 62-71% ethanol, 0.5% hydrogen peroxide, or 0.1% sodium hypochlorite inactivated the HCoVs within one minute [14]. Several methods, for instance, high temperature (including autoclaving at 121^{0}C) [21,22], heat [23,24], sunlight [25], 70% ethanol [26,27], microwave irradiation [28], detergents [23], trizol reagent [23], ozone [29], vaporized hydrogen peroxide [30], and gamma/UV radiations [31–33] have been implemented for rapid inactivation of SARS-CoV-2-contaminated surfaces. In 2017, the WHO developed and recommended two alcohol-based hand rub formulations, WHO-I (80% ethanol-1.45% glycerol-0.125% hydrogen peroxide) and II (75% isopropyl alcohol-1.45% glycerol-0.125% hydrogen peroxide) against Ebola virus, human Influenza A virus, and Modified vaccinia Ankara strain [34]. In a study by Kratzel *et al*, both of these hand rub formulations demonstrated potent virucidal activity against SARS-CoV-2, providing another effective tool for individual preventive care [26]. Consistent and robust evidence from many studies emphasizes that the use of respirators decreased the risk of infection in SARS-CoV-2 [35,36]. Several federal agencies, including the Center for Disease Control and Prevention (CDC), National Institute for Occupational Safety and Health (NIOSH), Food and Drug Administration (FDA), and Occupational Safety and Health Administration (OSHA), recommended the use of surgical masks and N95 filtering facepiece respirators (FFRs), along with gowns, eyeprotection, and gloves to prevent the spread of respiratory SARS-CoV-2 infection in the health care setting [37].

In response to the global COVID-19 pandemic and dwindling supplies of PPE [38], the WHO recommended a 40% increase in the production of PPE, especially surgical masks and N95 FFRs [12]. Increased demand for surgical masks, N95 FFRs and other PPE has resulted in a need for repeated usage of single-use disposable PPE and routine decontamination, as a crisis capacity strategy, with focus towards disinfection technologies [39]. Although FFRs are essential to protect from airborne viruses, the use of a contaminated FFR could potentially serve to self-inoculate or spread the virus to patients or other healthcare workers. Existing decontamination strategies of PPEs include ultraviolet germicidal irradiation (UVGI) [33,40,41], heat sterilization [42,43], chemical disinfectants [44], microwave radiation [41,42], and vapor phase hydrogen peroxide [45,46]. While these methods can effectively reduce pathogen load, material damage such as that caused by heat sterilization, peroxide vapor treatment, microwave irradiation, and chemical disinfectants may result in poor fit, reduced

 doi:10.20944/preprints202102.0078.v1

filtration efficiency and breathability which will in turn increase the wearer's potential exposure to pathogens [33,47,48]. This has lead to a demand for standardized, sustainable decontamination systems.

In this context, we sought to evaluate the efficacy of FATHHOME's ozone-based dry disinfection technology towards surface inactivation of HCoVs. Our data demonstrated that the decontamination environment provided by FATHHOME's portable ozone-based "dry sanitizer" is highly effective in inactivating human coronavirus, HCoV-OC43, by reducing the viral genomic RNA stability and virus infectivity. HCoV-OC43 (Biosafety level-2+/BSL-2+ pathogen), is a betacoronavirus which causes respiratory illness among infected individuals [49]. Given the high similarity of HCoV-OC43 to SARS-CoV-2 (BSL-3+ pathogen), lower infectious risk, and presence of lower-containment laboratory, it is feasible to use HCoV-OC43 as a SARS-CoV-2 surrogate, to determine the efficacy of ozone gas in virus disinfection [50]. Our results demonstrated that even a brief ozone exposure, 20 ppm for 10 min, can effectively eliminate 99.8-99.9% of infectious virus on solid and porous surfaces, while maintaining ambient ozone concentrations below 0.01ppm during the entirety of the sanitization cycle. Additionally, the efficacy of ozone in inactivating the virus was retained on dried virus, suggesting a broader application for cleaning and disinfection in essential public and healthcare facilities. In summary, this study provides conclusive experimental evidence that FATHHOME's ozone-based disinfection results in a 6-log reduction in viral viability and could be adopted to decontaminate various environmental surfaces, PPE and personal items, containing wet and dry films of virus, in the presence of biological fluids.

2. Materials and Methods

2.1. Cells

The human lung adenocarcinoma NCI-H441 cells were purchased from ATCC and maintained in RPMI medium supplemented with 10% fetal bovine serum (FBS, Atlanta Biologicals), 2 mM L-glutamine, 25 U/mL penicillin, and 25 µg/mL streptomycin. The A549-hACE2 (HA-Flag) cells were obtained from BEI Resources and maintained in Dulbecco's modified Eagle medium (DMEM) supplemented with 10% fetal bovine serum (FBS, Atlanta Biologicals), 2 mM L-glutamine, 25 U/mL penicillin, and 25 µg/mL streptomycin and 1ug/mL puromycin. The cells were grown at 37^{0}C and 5% CO_2 in a humidified chamber.

2.2. Human coronavirus

HCoV-OC43 strain, is a human coronavirus and belongs to the family *Coronaviridae*, genus betacoronavirus. HCoV-OC43 was obtained from BEI Resources (NIAID, NIH) and propagated in NCI-H441 cells by infecting the cell monolayer with the virus for 2 h at 34^{0}C. Unattached virus was removed by washing followed by addition of fresh medium. After 4 days, supernatant containing virus was harvested, cell debris were removed by centrifugation and the virus was aliquotted, and stored at -80^{0}C until further use. Viral copies in the harvested supernatant were quantified by Reverse Transcriptase qPCR (RT-qPCR) using a standard curve (described later in *2.3. RNA extraction and qPCR*) as well as infectivity assay and the detection of virally infected cells through immunofluorescence assay. All the assays were performed under BSL-2+ containment.

2.3. RNA extraction and qPCR

For the detection of viral genomic RNA through RT-qPCR, control or ozone-treated virus from the supernatant (for intact viral genomic RNA) or from infected A549-hACE2 (HA-FLAG) cells (for infectious viral genomic RNA) were subjected for total RNA extraction using Trizol reagent (Invitrogen, Carlsbad, CA), according to the manufacturer's recommendation. An aliquot of extracted total RNA (1 µg) was used for synthesizing the cDNA using high capacity RNA to cDNA kit (Invitrogen, Carlsbad, CA). A fraction of synthesized cDNA (5 µL) was used for the relative quantification of viral genomic copies using OC43-SF 5'-GGCTTATGTGGCCCCTTACT-3' and OC43-SR 5'-GGCAAATCTGCCCAAGAATA-3' primer set in a RT-qPCR assay (ThermoFisher

 doi:10.20944/preprints202102.0078.v1

Scientific, Waltham, MA). 10-fold serial dilutions of HCoV-OC43 genomic RNA (BEI Reourses, cat.# NR-52727 with $2.0x10^8$ genome equivalents/ml) were used for generating a standard curve to quantify the HCoV-OC43 viral copies in the virus preparations.

2.4. Virus Infectivity through Immunofluorescence Assay

Control or ozone-treated viruses were added onto the human lung carcinoma, A549-hACE2 (HA-FLAG) cells for 2h (34^0C, 5% CO_2). Following infection, the cells were incubated for 48h at 34^0C in a humidified chamber supplemented with 5% CO_2. Infected cells were detected by using the immunofluorescence assay (IFA) of the nucleocapsid protein of HCoV-OC43 (Millipore Sigma). Infected cells were fixed using 3.2% formaldehye and permeabilized with 0.1% Triton X-100 for 10 min, washed (2x) and blocked (0.4% FSG-0.05% Triton X-100) for 45 mins at room temperature. Cell monolayers were washed (2x) and incubated with monoclonal mouse anti-HCoV-OC43 nucleocapsid antibody (1:1000; Millipore Sigma) overnight at 4^0C, followed by incubation with chicken anti-mouse Alexa Fluor 594 (1:1000; Molecular Probe, Carlsbad, CA), secondary antibody for 1h at RT in the dark. Finally, the nuclei were stained with DAPI (1:7000; ThermoFisher, Walthman, MA). Coverslips were mounted on the glass slides using prolong diamong antifade (ThermoFisher) and the slides were examined using Carl Zeiss LSM 780 microscope.

2.5. FATHHOME Device

FATHHOME'sportable, ozone-based dry sanitization device is equipped with a patented vacuum-sealed chamber, computer-controlled ozone generator, and catalytic (MnO_2/CuO_2) converter system. The device cycles the internal pressure between -30kPa and -15 kPa which permeates ozone throughout the chamber whileensure none of it escapes during the sanitization cycle . Once the vacuum seal is generated, Ozone is produced by the device at point-of-use using electricity and atmospheric air, through cleavage of O2 into elemental oxygen (which combines with molecular oxygen (O2) to create transient O3) via a corona discharge device. The system then back-fills the evacuated chamber with air while maintaining target ozone concentration levels (20ppm, 25ppm, 50ppm). At all times, the contents of the chamber are being held under negative pressure with all gases in the chamber being pumped through the manganese dioxide/copper oxide ozone scrubber to ensure environmentally safe device exhaust within OSHA and FDA guidelines. . The FATHHOME device can be operated through its onboard microcontroller which is accessed either via a switch located on the device or via a cloud-based web-panel. For the duration of this study, the FATHHOME device was kept inside BSL-2+ containment and controlled remotely outside the test room for each disinfection cycle.

2.6. Experiment Set up

In order to test the efficacy of ozone in accelerating the inactivation of HCoV-OC43 using FATHHOME's dry sanitizing device, 100 µL of the virus stock (equivalent to $2.1x10^6$ calculated viral particles) were applied as 10 x 10 µl liquid droplets on top of glass coverslips (ThermoFisher, 18mm diameter), and N95 FFRs (ThermoFisher, $1cm^2$ square pieces), each placed in the center of a well of 12-well culture plate (Fig. 1), kept inside the BSL-2+ containment.

Preprints (www.preprints.org) | NOT PEER-REVIEWED | Posted: 2 February 2021 doi:10.20944/preprints202102.0078.v1

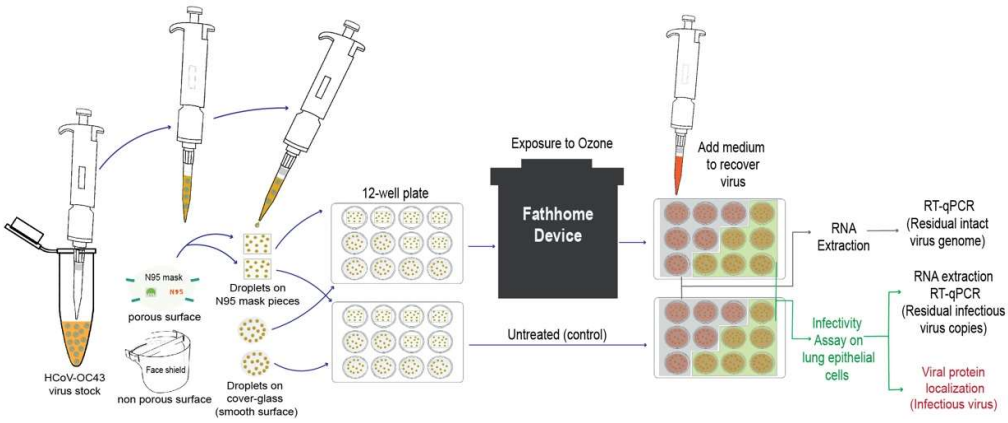

Figure 1. Schematic representation of the experimental set up utilized for the evaluation of ozone based inactivation of HCoV-OC43 using FATHHOME device. An aliquot (100 µl) with known amounts of HCoV-OC43 virions was placed on the chosen surface (glass coverslips and N95 FFR), and exposed to ozone for indicated exposure dose and time. The mock- and ozone-treated viruses were then collected to determine the viral RNA stability (via quantitative RT-PCR), and viral infectivity, which involves detection of infectious intracellular RNA copies (via qRT-PCR) and localization of viral protein (through IFA) in A549-hACE-2 (HA-FLAG) cells.

The applied virus was present in the culture medium containing fetal bovine serum, providing proteinaceous content resembling the composition of nasal secretions or respiratory droplets. The virus-containing 12-well plate was placed inside the FATHHOME device (at the center) and exposed to varying doses of ozone gas (20, 25 and 50 ppm) for specified times (10, 15, and 20 mins). The sanitizing chamber's ozone-gas concentration level was monitored during each disinfection cycle using a NIST Calibrated ozone sensor (FD-600-O3 Ozone Analyzer, Forensics Detectors, CA) connected directly to a 3/32" sensor port on the FATHHOME device's vacuum chamber. The FD-600-O3 features a built-in extraction pump that allows it to detect 0-100 ppm ozone with 0.1 ppm resolution under both atmospheric and vacuum pressure conditions. This data was logged to csv over a Serial-USB interface at a sampling rate of 1 measurement per second. Any residual ozone gas leakage during the ozone disinfection cycle was measured (on-screen) using a second ozone gas sensor (Porta Sens II, ThermoFisher, MA) placed in the BSL-2+ containment next to the FATHHOME device. All the experiments were conducted at 25^{0}C and 45% relative humidity (standard indoor humidity), as measured with AcuRite Indoor Thermometer and Hygrometer with Humidity Gauge (Acurite, Inc.). Virus-laden glass coverslips and N95 FFRs without ozone treatment served as a control for calculating viral inactivation efficiencies. In addition, the efficacy of HCoV-OC43 inactivation when the virus is present as a dried droplet on the chosen surface was evaluated by drying the virus (HCoV-OC43) as small (10 µl) liquid droplets inside the FATHHOME device before exposing to ozone gas. For drying, 10 x 10 µl liquid droplets for a total of 100 µl, were deposited on glass coverslips and N95 FFRs and subjected to a cyclical vacuum drying routine inside the FATHHOME device for 1 min or 10 mins, at 25^{0}C and 45% humidity, before ozone exposure. After each disinfection cycle, the mock-treated and ozone-treated viruses were recovered by adding 500 µl of culture medium on the surfaces and allowing it to resuspend, for 15 min at 34^{o}C. The recovered viruses were either collected in a 1.5 mL eppendorf tube for further extraction of total viral RNA with Trizol reagent for viral genome quantitation using qRT-PCR or applied onto a permissive A549-hACE2 HA-FLAG cell monolayer for the detection of residual infectious virus through integrated cell culture PCR and localization of infected cells through immunofluorescence assay (Fig. 1). The A549-hACE2 (HA-FLAG) cells are a human lung carcinoma (A549) cell line over-expressing human angiotensin converting enzyme-2 (hACE-2) under control of the XYZ promoter. Each assay was done in duplicates and each experiment was conducted three independent times.

Preprints (www.preprints.org) | NOT PEER-REVIEWED | Posted: 2 February 2021 doi:10.20944/preprints202102.0078.v1

2.7. Statistical analysis

Data presented are an average of three independent experiments and the error bars represent the standard deviation across independent experiments. Statistical analyses were performed using Prism 8.0 software (Graphpad Inc.) and the p-values were calculated using 2-way ANOVA and the p-value cut offs for statistical significance were *, $p<0.1$; and **, $p<0.01$.

3. Results

3.1. Assay development to quantify infectious HCoV-OC43

In order to quantify infectious virus, we utilized an integrated cell culture PCR assay and the detection of infected cells by quantifying viral genomic RNA and by localizing HCoV-OC43 nucleocapsid protein through immunofluorescence of infected cells. Varying amounts of HCoV-OC43

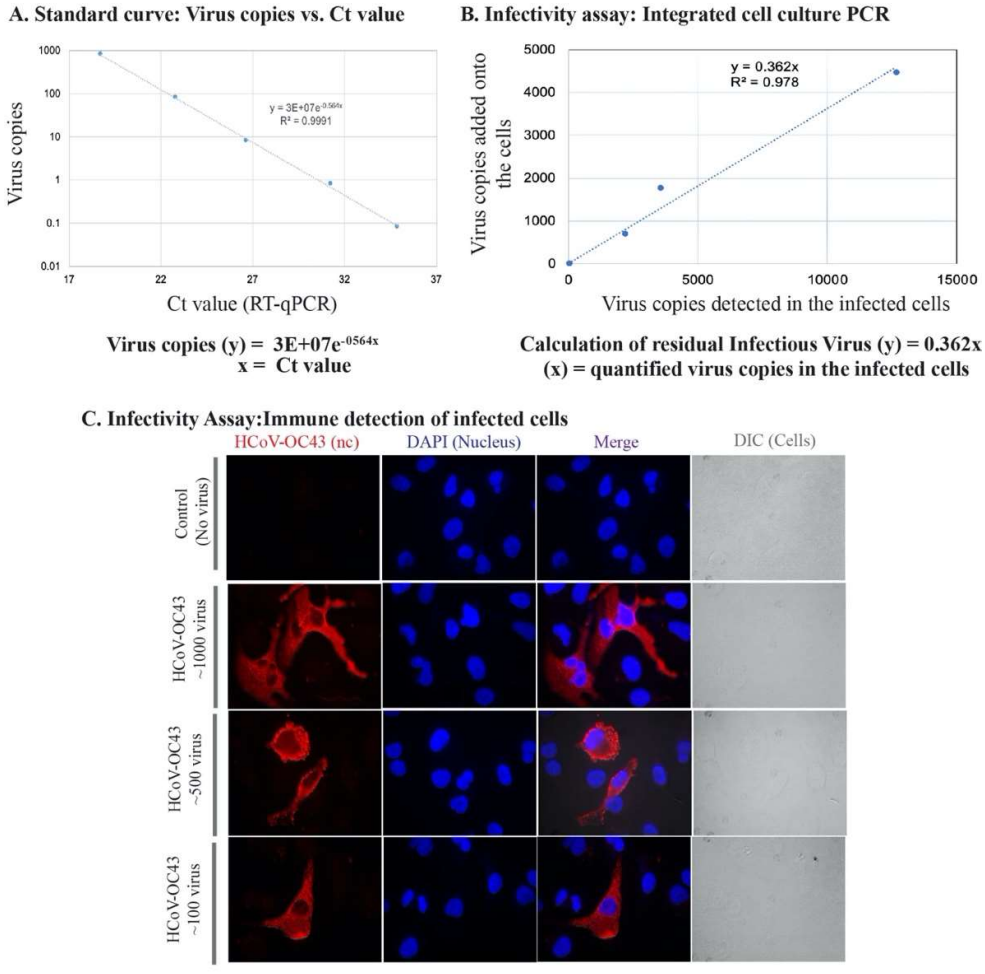

Figure 2. Assay establishment: Integrated cell culture PCR and Immuno detection of HCoV-OC43 infected cells. **A.** Standard curve of varying HCoV-OC43 genome copies with Ct value. **B.** Correlation of HCoV-OC43 viral copies added onto A549-hACE2 cells and detection of intracellular viral genome copies following infection and replication. **C.** Immune localization of HCoV-OC43 nucleocapsid protein in A549-hACE2 cells infected with varying amounts of virus. Nucleocapsid was detected with anti-HCoV-OC43 antibody followed by staining with chicken anti-mouse Alexa Fluor 594 (red). Nuclei were stained with DAPI (blue). DIC images are to show cell morphology.

virus, calculated using a standard curve (Fig. 2A) from our stock were added onto a permissive cell line, A549-hACE2 (infectivity assay) followed by the detection of viral genome copies after a 48h

 doi:10.20944/preprints202102.0078.v1

incubation. We detected a strong correlation between the amount of viral genome copies detected and the amount of virus copies added onto the cells (R^2=0.978) (Fig. 2B). We also confirmed the infectivity of our virus stock and the detection of viruses in the infected cells by adding different quantities of viral particles on A549-hACE2 and localizing HCoV-OC43's nucleocapsid using immunofluorescence antibody staining. Lack of any signals in control (uninfected cells) and specific localization of nucleocapsid signals confirmed the specificity of our assay (Fig. 2C). Further, cells infected with lower amounts of HCoV-OC43 virus showed reduced number cells with nucleocapsid detection, as expected (Fig. 2B).

3.2. Effect of ozone exposure on HCoV-OC43 virus stability on different surfaces

The FATHHOME dry sanitization device is based on antimicrobial ozone technology, and has been previously shown to inactivate more than 99% of *E. coli* bacterium on contaminated fabric [51]. In an attempt to test the disinfection efficiency of FATHHOME on HCoVs, HCoV-OC43 was used as a surrogate of the highly contagious SARS-CoV-2 for practical reasons. Given the high genomic sequence similarities between betacoronavirus family members, human cell entry and infection mechanisms as well as inactivation conditions are likely to be similar [52]. In this study, we tested the virus decontamination on two different surfaces, i.e. a nonporous smooth surface (glass coverslips) and a porous soft surface (N95 FFRs). HCoV-OC43 virus suspensions (10 x 10 µl liquid droplets) were applied onto each surface and placed inside a 12-well plate. The plate containing HCoV-OC43 viruses was exposed, after removing the lid, to an ozone concentration of approx. 20 ppm and an ambient pressure of 68kPa to 85kPa produced by the FATHHOME device, situated inside a BSL-2+ containment for 10 min (Fig. 3A). Glass coverslips and N95 FFRs containing a same amount of virus without ozone treatment were used as a control in our assay. Untreated and ozone-treated viruses were collected for the evaluation of virus inactivation by direct genomic RNA quantitation (RT-qPCR) and infectivity assay using permissive A549-hACE2 cells. Presence of the viral genomic RNA was determined using RT-qPCR as used earlier for detection of SARS-CoV-2 in environmental surface and air samples [17]. Detection of genomic viral RNA through RT-qPCR is considered to be a highly sensitive method for the detection of viral genomic RNA, however, a positive result doesn't necessarily mean that viral genomic RNA is intact or that the RNA is inside an infectious virus. However, absence of a virus specific PCR signal confirms absolute removal of virus and viral genome. Therefore, viral genomic RNA quantitation along with infectivity assays was devised for estimating viral inactivation efficacies. HCoV-OC43 viral copies in the ozone treated and untreated samples were calculated based on the standard curve generated using serial dilutions of known HCoV-OC43 genomic RNA (Fig. 2). The intact residual virus copies in ozone-treated samples were calculated and compared to the untreated controls, set to 100%. As expected, the copies of viral genomic RNA declined (i.e. one $\log_{10}$ decrease) after a 10 minutes, 20 ppm ozone-exposure on both the tested surfaces (Fig. 3B). Interestingly, we saw a slightly higher reduction (98.14%) in the viral genomic RNA on N95 FFRs, than glass coverslips (90.71%) in this assay (Fig. 3B).

In order to determine residual infectious virus, untreated control and ozone exposed HCoV-OC43 viruses were added onto the A549-hACE2 cells for 2 h at 34^{0}C to facilitate attachment and entry of the residual live virus. The over-expression of ACE-2, the entry receptor for HCoVs including, HCoV-NL63, SARS-CoV, and SARS-CoV-2, facilitates the entry of HCoV-OC43 into the cells [53]. Quantitation of intracellular HCoV-OC43 genome copies through spike glycoprotein gene specific RT-qPCR led to the calculation of infectious virus added onto the target cells as described in Fig. 2B. Calculated residual live virus copies based on the intracellular viral genomic copies, showed that ozone effectively reduced the amounts of infectious virus when compared with the control, non-ozone treated samples. Noticeably, there was a higher, 99.49% reduction (Fig. 3C), in infectious virus on smooth surface, than from soft surface (96.78% reduction). These observed differences could be attributed to surface composition variability, which affects virus adsorption and infectivity. Additionally, presence of live virus was detected by localizing the viral nucleocapsid protein through immunofluorescence staining for HCoV-OC43 viral protein (Fig. 3D). As shown in Fig. 3D, addition of ozone-exposed HCoV-OC43 virus resulted in a reduction of the virus-positive cells, compared to

Preprints (www.preprints.org) | NOT PEER-REVIEWED | Posted: 2 February 2021 doi:10.20944/preprints202102.0078.v1

the untreated controls where 95% of cells were positive for HCoV-OC43 protein. In contrast, for ozone-exposed virus, we only observed 5 and 14 cells stained positively for HCoV-OC43 protein (out of 500 cells) after virus recovery from the glass and N95 FFRs surfaces, respectively. Overall, these results indicate that ozone is effective in inactivating human coronavirus.

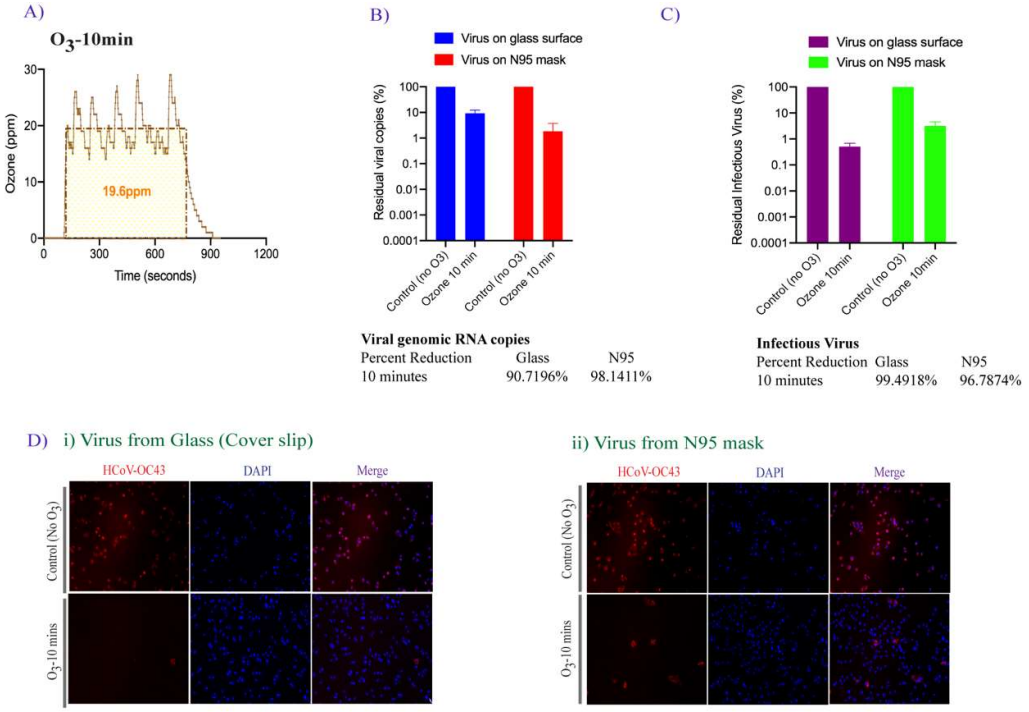

Figure 3. The effect of 20 ppm-10 min ozone exposure on HCoV-OC43 viral genomic RNA stability and infectivity. **A.** The plot depicting the average ozone dose (20 ppm-10 min) generated via FATHHOME device to which the virus was exposed. The ozone dose data was recorded using the connected FD-600-O3 ozone detector. **B.** HCoV-OC43 virus (10 x 10 µl droplets) was applied on coverslips and N95 FFRs, and exposed to 20 ppm ozone gas for 10 min. Total RNA was extracted and used for the detection of viral copies by RT-qPCR. **C.** HCoV-OC43 virus (100 µl) was exposed to 20 ppm-10 min ozone treatment, collected and used for the infection of A549-hACE-2 cells. Total RNA was extracted 48h post-infection for the detection of intracellular viral genomic copies in a RT-qPCR assay. Viral copies were calculated based on a standard curve generated using the known amounts of virus (BEI Resources), and quantified with respect to untreated controls, set to 100%. **D.** Untreated and ozone-treated HCoV-OC43 virus infected A549-hACE-2 cells were fixed and immunostained with HCoV-OC43 antibody (for nucleocapsid protein) for immunofluorescence assay. Virus internalization showed virus preferably localized on the membrane (red signals) in HCoV-OC43 infected cells. Nuclei were stained with TO PRO-3 (blue signals). The uninfected and infected cells were identified and quantified using automated Image J macro method.

3.3. Effect of increased contact time of ozone exposure on HCoV-OC43 virus inactivation

We next examined the possibility of improving viral inactivation and viral genome degradation by exposing the surfaces containing virus containing droplets to increasing levels of ozone and exposure time. The surfaces were exposed to 25 ppm ozone and an ambient pressure of 68kPa to 85kPa for 10, 15, and 20 mins (Fig. 4A). The recovered virus was either evaluated for viral genome RNA stability (using qRT-PCR) or added onto the cells for residual infectious virus quantification using RT-qPCR and immunofluorescence assay as described above. Surprisingly, an increase in ozone exposure to 25 ppm for 10 min did not significantly change the number of intact viral genomic copies on both, smooth or porous surfaces (Fig. 3 and 4 panel B). In contrast, increasing the ozone contact time (from 10 to 15 mins) dramatically enhanced the degradation of HCoV-OC43 virus (4-

Preprints (www.preprints.org) | NOT PEER-REVIEWED | Posted: 2 February 2021 doi:10.20944/preprints202102.0078.v1

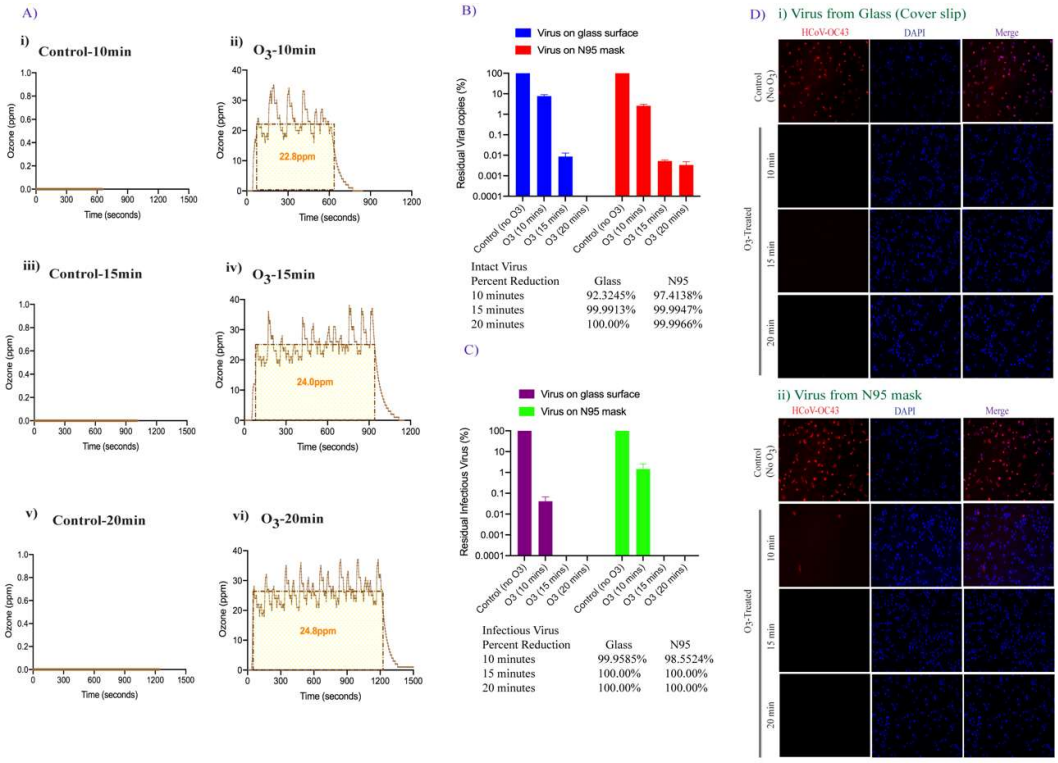

Figure 4. FATHHOME's ozone dose-response assessment of HCoV-OC43 inactivation. **A.** The ozone (ppm) vs time (sec) plot showing the average ozone gas to which the virus was exposed during ~25 ppm-10, 15, and 20 min ozone treatment, as generated via FATHHOME device. **B.** HCoV-OC43 virus aliquot (100 µl) was placed on glass coverslips and N95 FFRs and exposed to 25 ppm of ozone for 10, 15- and 20-min. Following ozone treatment, HCoV-OC43 was collected for viral RNA extraction. Intact residual viral copies were calculated based on the standard curve. **C.** HCoV-OC43 virus was collected post ozone treatment, for virus infectivity and replication, and subjected to the infection of A549-hACE-2 cells. Intracellular infectious RNA copies were determined through RT-qPCR and viral copies were calculated based on the standard curve and quantified with respect to untreated controls, set to 100%. **D.** HCoV-OC43 infection and replication in untreated and ozone-treated HCoV-OC43 virus infected cells was detected by immune localization of HCoV-OC43 nucleocapsid protein through IFA (red signals). Nuclei were stained with TO PRO-3 (blue signals). The quantification of cells was done using automated Image J macro analysis.

fold, 99.99% reduction) and a further increase in the contact time (from 15 to 20 mins) led to complete degradation of viral genomic RNA on smooth surfaces (Fig. 4B). For N95 FFRs, increasing the contact time of 25 ppm ozone exposure from 10 to 15 mins, also resulted in a 99.99% HCoV-OC43 reduction, and increasing exposure time to 20 minutes did not further decrease viral genomic RNA (Fig. 4B). Since the RT-qPCR detects any traces of viral genome even from already inactivated virus particles, we further determined the copies of infectious virus using the infectivity assay. Recovered virus after ozone treatment were added onto A549-hACE2 cells for residual infectious virus to infect the cells and replicate for 48h. Estimation of residual infectious viral copies for 25 ppm-10 min ozone treatment, through RT-qPCR confirmed lower copies of the infectious virus (three $\log_{10}$ reduction) were recovered from smooth surface as compared to virus recovered from soft surface (one $\log_{10}$ reduction, Fig. 4C). Further, the HCoV-OC43 virus had been completely degraded (below the detection limit) on both the surfaces after 15 and 20 min exposure of 25ppm ozone. These results confirmed that surface disinfection of coronavirus can be achieved quickly and safely and that ozone dose and contact time can further enhance the sterilization activity. The results from the infectivity assay, detecting HCoV-OC43 infected cells, with ozone treated and untreated virus correlated well with the qRT-PCR results (Fig. 4D). Absence of any HCoV-OC43 protein stained A549-hACE2-cells,

 doi:10.20944/preprints202102.0078.v1

as compared to untreated control virus, further confirmed complete HCoV-OC43 inactivation 10, 15, and 20 min after 25 ppm-ozone treatment on smooth surface. Although we detected 1.6% HCoV-OC43 protein positive cells (8 positive cells out of 500 cells examined) in virus recovered from N95 mask exposed 10min after 25 ppm exposure, an increase in the ozone exposure time to 15min completely abrogated infectious virus copies (Fig. 4D). As expected, no residual live virus could be detected 20 min after 25 ppm ozone exposure (Fig.4D).

3.4.Doubling the ozone concentration reduced exoposure time to achieve faster virus inactivation.

We further determined whether increasing the ozone concentration can reduce the exposure time necessary for complete disinfection of HCoV-OC43 virus. To this end, the same amounts of HCoV-OC43 coronavirus were applied onto coverslips and N95 FFRs placed inside the wells of a 12-well plate and exposed to 50 ppm ozone gas and an ambient pressure of 68kPa to 85kPa for 10, 15, and 20 mins (Fig. 5A). Total RNA was extracted to quantify the intact genomic HCoV-OC43 RNA copies through RT-qPCR, as described above. As expected, prolonged exposure of the surfaces to 50 ppm ozone disintegrated 99.9% of virus genomic RNA (3-fold reduction) within 10 min of exposure, on both the tested surfaces (Fig. 5B). Increasing the exposure time to 15 minutes did not further reduce the viral copy load detected on glass surfaces or N95 FFRs. Furhter increasing the exposure time to 20 minutes at 50 ppm ozone, resulted in no residual intact viral genomic copies detected on either glass surfaces or N95 FFRs. The recovered viruses from both the surfaces were subsequently assayed for virus infectivity using A549-ACE2 cells, and the results are shown in Fig. 5C. The RT-qPCR analysis for residual live virus quantification, showed a complete disintegration of the viral genome (below the detection limit), present on both the tested surfaces, regardless of the exposure time (Fig. 5C). The virus infectivity was also analyzed using IFA (Fig. 5D). No residual infectious virus was detected in the virus culture assays for all the selected time points. Thus, the FATHHOME device can safely operate under OSHA and FDA ozone emissions limits at an internal ozone concentration of 50 ppm leading to 100% inactivation of HCoV-OC43 virus within 10 mins.

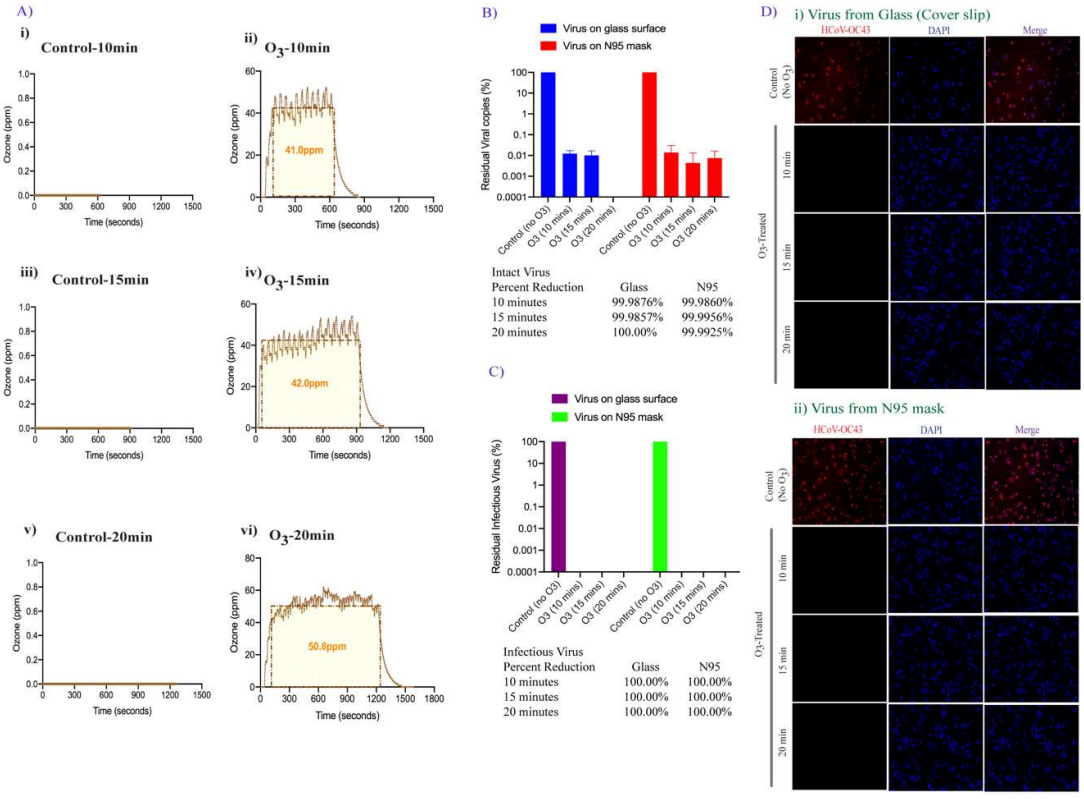

 doi:10.20944/preprints202102.0078.v1

Figure 5. Effect of higher ozone dose on HCoV-OC43 inactivation. **A.** The ozone (ppm) vs time (sec) plot depicting the ozone sensor readings when the virus was subjected to ~ 50 ppm-10, 15, and 20 min of ozone exposure, as generated via FATHHOME device. **B.** HCoV-OC43 virus aliquot (100 µl) was placed on glass coverslips and N95 FFRs and exposed to 50 ppm of ozone for 10, 15- and 20-min. Following ozone treatment, HCoV-OC43 was collected for viral RNA extraction, followed by quantitation of the intact residual viral copies based on the standard curve. **C.** Following ozone exposure, HCoV-OC43 virus was collected, and subjected to the infection of A549-hACE-2 cells. Relative intracellular infectious RNA copies were calculated through RT-qPCR based on the standard curve and quantified with respect to untreated controls, set to 100%. **D.** Uninfected and infected cells were counted using the automated Image J macro analysis. HCoV-OC43 infection was detected by immune localization of HCoV-OC43 nucleocapsid protein through IFA (red signals). Nuclei were stained with TO PRO-3 (blue signals).

4. Discussion

In the past few years, four major respiratory viruses, including Influenza A viruses, SARS-CoV, MERS-CoV, and now SARS-CoV-2, have lead to global infectious disease outbreaks and an international public health emergency. These epidemics/pandemics include Spanish influenza (1918), Asian influenza (1957), Hong Kong flu (1968), novel influenza A virus (2009), SARS-CoV (2003), MERS-CoV (2012), and novel SARS-CoV-2 (2019) [54,55]. Interestingly, the airborne transmission of respiratory viruses through direct or indirect contact or even without contact over a distance contributes to the associated respiratory infections being ubiquitous [56]. The widespread dissemination and survival of respiratory viruses on infected surfaces or individualized items, and the severity of infection, highlight the need of reviewing available as well as establishing newer decontamination approaches to control the spred of infections. Although, masks, personal protective equipment, distancing, and disinfecting appear effective in controlling exposure to infections, the ongoing SARS-CoV-2 pandemic and potential future epidemics, call for the development of new viral deactivation technologies to help control the virus spread. Thus an urgent need remains to develop and validate virus deactivation technologies to provide rapid, effective and safe decontamination solutions. Hence, in this study, we validated the surface inactivation of human coronavirus HCoV-OC43, a less-pathogenic model of SARS-CoV-2, using FATHHOME's high-volume, eco-friendly, ozone-based dry sanitizing system.

Ozone, a triatomic oxygen molecule, is a potent oxidizer shown to possess anti-microbial properties [57]. Ozone is created via dissociation of oxygen molecules into atomic oxygen, which then quickly combines with other oxygen molecules to form ozone [58]. Ozone is an effective disinfectant against bacteria [59,60] and viruses [61,62] including enveloped HCoVs [63–66]. A study on efficacy of ozone solution disinfectant in inactivating SARS-CoV has shown a high dose of ozone (27.73mg/L) could kill the virus in 4 mins [67]. Anti-microbial activity of ozone towards virus inactivation of surfaces has also been demonstrated using bacteriophages ϕX174, MS2, ϕ6 and T7, as surrogates of mammalian viruses [63], and nosocomial bacterial pathogens including Clostridium difficile, Acinetobacter baumanii and Staphylococcus aureus [68]. Although, the mechanism of anti-viral activity of ozone is yet to be fully understood, ozone deactivates virus through both the direct (ozone) and/or indirect (generation of reactive oxygen species/ROS) reaction mechanisms [69]. The viral proteins of HCoVs are susceptible to oxidative damage by ozone due to the presence of oxidation-prone amino acids (tryptophan, methionine, and cysteine due to sulfhydryl residues, R-S-H), and the fatty acids (arachiodonic acid, linoleic acid, and oleic acid due to unsaturated bonds), alterations in which affects the viral protein's structure, biochemical activity and virus growth properties. Fragmentation of viral proteins allows ozone to attack and damage viral nucleic acid making it non-infectious [70]. Due to its excellent oxidizing properties, aqueous ozone has been extensively used to disinfect water, purify air, and preserve food [71], however, the use of ozone gas on a commercial level still needs to be explored. Ozone in its gaseous state allows better penetration and inactivation of contaminated surfaces (both porous and nonporous) more effectively than liquid disinfectants.

Interestingly, ozone gas generated via FATHHOME's dry sanitizing system effectively inactivated HCoV-OC43 (>99% reduction) under all tested conditions. Recently, Dubuis *et al* have demonstrated that maximum anti-viral efficacy of ozone against airborne viruses requires a low dose

of the ozone gas exposure combined with a high relative humidity [65]. In another study, aimed to design a mobile ozone generator for deactivating viruses, 20-25ppm ozone coupled with >90% relative humidity was found effective in achieving at least three $\log_{10}$ virus reduction in all 12 tested viruses [72]. In both studies, the effect of the increased relative humidity was studied and shown to augment the virucidal properties of ozone. In our study, we have demonstrated that HCoV-OC43 is susceptible to oxidative damage by ozone. An interesting finding is that using FATHHOME's device 20-25ppm ozone exposure for 10-15 min, can completely eliminate HCoV-OC43 virus on both coverslips and N95 FFRs (more than 6 $\log_{10}$ reduction) even at ambient relative humidity (45%). Since FATHHOME can maintain ozone's antiviral efficacy in a typical air-conditioned environment (25^0C and 45% relative humidity), it may find important and broader practical applications.

Surgical masks and N95 FFRs prevent workplace exposure to SARS-CoV-2 in essential healthcare and non-healthcare settings [44]. Concerned by the pandemic potential of COVID-19, use of face masks, surgical masks (to filter infectious particles spreading via droplets), and N95 FFRs (to filter at least 95% of particulates), became mandatory in nearly all COVID-19 affected countries. A rise in the global demand has resulted in a shortage of disposable surgical masks and N95 FFRs. Consequently, reuse of single-use disposable masks has been implemented although there is no standard decontamination protocol for safe decontamination and reprocessing of the masks although UVGI, moist heat, microwave-generated steam, and vaporized hydrogen peroxide seem to be the current standard for N95 decontamination [33,37,40–43]. Although, all these methods have advantages and disadvantages, a careful consideration of the type of respirator and biological target has to be performed, to restore the fit and filtration capacity of the N95 respirator post decontamination.

FATHHOME's dry sanitizing technology can quickly and gently sanitize articles not compatible with traditional chemical-based disinfectants, "wet" sanitization methods, or methods involving heat and pressure. Such technology is particularly relevant to frontline workers outside the hospital setting (smaller medical/dental offices, EMS, fire and police stations, home care nurses, staff at long term care homes, retail workers, the food and hospitality industry) that produce significant amounts of daily medical and PPE waste to keep their workforce safe, but do not have access to expensive industrial-scale sanitization systems. In addition, workers are now faced with "decontamination fatigue" as time-consuming (and often ineffective) decontamination tasks, which they thought were temporary, have now become part of daily routines.

In the past 25 years, 15 major global outbreaks of airborne infectious diseases have occurred, including notable outbreaks of Influenza H1N1 in 2009 and the SARS and MERS coronaviruses in 2002-2003 2012, respectively. In a world of 7.8 billion people, environmental changes, inadequate global access to healthcare, and an interconnected global marketplace suggest that the emergence of SARS-CoV-2 will not be the last pandemic. The adoption of accessible, easily-deployable, rapidly-scalable, and environmentally conscious decontamination systems will balance the need for safety against the challenges of a post-pandemic world.

Author Contributions: S.C.V. was the lead scientist of the project and supervised the research. T.U. performed the experiments and data analysis. T.U., A.K., A.M.S., S.C.V. wrote the paper and participated in discussions and data interpretation.

Funding: The research performed at UNR described in this manuscript received no external funding and was carried out using institutional resources. A.M.S. was supported by the Dept of Energy, Office of Technology Transitions under the COVID Technical Assistance Program.

Acknowledgments: Human Coronavirus, OC43 (HCoV-OC43) was obtained through BEI Resources, NIAID, NIH: Human Coronavirus, OC43, NR-52725..

Conflicts of Interest: The authors declare no conflict of interest.

References

1. Ye, Z.-W.; Yuan, S.; Yuen, K.-S.; Fung, S.-Y.; Chan, C.-P.; Jin, D.-Y. Zoonotic Origins of Human Coronaviruses. *Int. J. Biol. Sci.* **2020**, *16*, 1686–1697, doi:10.7150/ijbs.45472.

2. Hu, B.; Guo, H.; Zhou, P.; Shi, Z.-L. Characteristics of SARS-CoV-2 and COVID-19. *Nat. Rev. Microbiol.* **2020**, doi:10.1038/s41579-020-00459-7.
3. Wei, W.E. Presymptomatic Transmission of SARS-CoV-2 — Singapore, January 23–March 16, 2020. *MMWR Morb. Mortal. Wkly. Rep.* **2020**, *69*, doi:10.15585/mmwr.mm6914e1.
4. Buitrago-Garcia, D.; Egli-Gany, D.; Counotte, M.J.; Hossmann, S.; Imeri, H.; Ipekci, A.M.; Salanti, G.; Low, N. Occurrence and Transmission Potential of Asymptomatic and Presymptomatic SARS-CoV-2 Infections: A Living Systematic Review and Meta-Analysis. *PLOS Med.* **2020**, *17*, e1003346, doi:10.1371/journal.pmed.1003346.
5. COVID-19 Map Available online: https://coronavirus.jhu.edu/map.html (accessed on 19 January 2021).
6. Oran, D.P.; Topol, E.J. Prevalence of Asymptomatic SARS-CoV-2 Infection. *Ann. Intern. Med.* **2020**, *173*, 362–367, doi:10.7326/M20-3012.
7. Wj, W.; A, R.; Ac, C.; Sj, P.; Hc, P. Pathophysiology, Transmission, Diagnosis, and Treatment of Coronavirus Disease 2019 (COVID-19): A Review Available online: https://pubmed.ncbi.nlm.nih.gov/32648899/ (accessed on 19 January 2021).
8. Gibson, P.G.; Qin, L.; Puah, S.H. COVID-19 Acute Respiratory Distress Syndrome (ARDS): Clinical Features and Differences from Typical Pre-COVID-19 ARDS. *Med. J. Aust.* **2020**, doi:10.5694/mja2.50674.
9. Archer Stephen L.; Sharp Willard W.; Weir E. Kenneth Differentiating COVID-19 Pneumonia From Acute Respiratory Distress Syndrome and High Altitude Pulmonary Edema. *Circulation* **2020**, *142*, 101–104, doi:10.1161/CIRCULATIONAHA.120.047915.
10. Badraoui, R.; Alrashedi, M.M.; El-May, M.V.; Bardakci, F. Acute Respiratory Distress Syndrome: A Life Threatening Associated Complication of SARS-CoV-2 Infection Inducing COVID-19. *J. Biomol. Struct. Dyn.* 1–10, doi:10.1080/07391102.2020.1803139.
11. Tojo, K.; Yamamoto, N.; Mihara, T.; Abe, M.; Goto, T. Characteristics of Changes in Circulating Markers of Alveolar Epithelial and Endothelial Injury in Acute Respiratory Distress Syndrome with COVID-19. *medRxiv* **2021**, 2021.01.10.21249528, doi:10.1101/2021.01.10.21249528.
12. A Review of Current Interventions for COVID-19 Prevention - PubMed Available online: https://pubmed.ncbi.nlm.nih.gov/32409144/ (accessed on 19 January 2021).
13. Stability of SARS-CoV-2 in Different Environmental Conditions - PubMed Available online: https://pubmed.ncbi.nlm.nih.gov/32835322/ (accessed on 19 January 2021).
14. Kampf, G.; Todt, D.; Pfaender, S.; Steinmann, E. Persistence of Coronaviruses on Inanimate Surfaces and Their Inactivation with Biocidal Agents. *J. Hosp. Infect.* **2020**, *104*, 246, doi:10.1016/j.jhin.2020.01.022.
15. Wang, W.; Xu, Y.; Gao, R.; Lu, R.; Han, K.; Wu, G.; Tan, W. Detection of SARS-CoV-2 in Different Types of Clinical Specimens. *JAMA* **2020**, *323*, 1843–1844, doi:10.1001/jama.2020.3786.
16. Tong, Y.; Bao, A.; Chen, H.; Huang, J.; Lv, Z.; Feng, L.; Cheng, Y.; Wang, Y.; Bai, L.; Rao, W.; et al. Necessity for Detection of SARS-CoV-2 RNA in Multiple Types of Specimens for the Discharge of the Patients with COVID-19. *J. Transl. Med.* **2020**, *18*, 411, doi:10.1186/s12967-020-02580-w.
17. Chia, P.Y.; Coleman, K.K.; Tan, Y.K.; Ong, S.W.X.; Gum, M.; Lau, S.K.; Lim, X.F.; Lim, A.S.; Sutjipto, S.; Lee, P.H.; et al. Detection of Air and Surface Contamination by SARS-CoV-2 in

Hospital Rooms of Infected Patients. *Nat. Commun.* **2020**, *11*, 2800, doi:10.1038/s41467-020-16670-2.

18. Moore, G.; Rickard, H.; Stevenson, D.; Aranega-Bou, P.; Pitman, J.; Crook, A.; Davies, K.; Spencer, A.; Burton, C.; Easterbrook, L.; et al. Detection of SARS-CoV-2 within the Healthcare Environment: A Multi-Centre Study Conducted during the First Wave of the COVID-19 Outbreak in England. *J. Hosp. Infect.* **2021**, *108*, 189–196, doi:10.1016/j.jhin.2020.11.024.
19. Kampf, G. Potential Role of Inanimate Surfaces for the Spread of Coronaviruses and Their Inactivation with Disinfectant Agents. *Infect. Prev. Pract.* **2020**, *2*, 100044, doi:10.1016/j.infpip.2020.100044.
20. Kampf, G. *Antiseptic Stewardship: Biocide Resistance and Clinical Implications*; Springer International Publishing, 2018; ISBN 978-3-319-98784-2.
21. Chen, H.; Wu, R.; Xing, Y.; Du, Q.; Xue, Z.; Xi, Y.; Yang, Y.; Deng, Y.; Han, Y.; Li, K.; et al. Influence of Different Inactivation Methods on Severe Acute Respiratory Syndrome Coronavirus 2 RNA Copy Number. *J. Clin. Microbiol.* **2020**, *58*, doi:10.1128/JCM.00958-20.
22. Grinshpun, S.A.; Yermakov, M.; Khodoun, M. Autoclave Sterilization and Ethanol Treatment of Re-Used Surgical Masks and N95 Respirators during COVID-19: Impact on Their Performance and Integrity. *J. Hosp. Infect.* **2020**, *105*, 608–614, doi:10.1016/j.jhin.2020.06.030.
23. Patterson, E.I.; Prince, T.; Anderson, E.R.; Casas-Sanchez, A.; Smith, S.L.; Cansado-Utrilla, C.; Solomon, T.; Griffiths, M.J.; Acosta-Serrano, Á.; Turtle, L.; et al. Methods of Inactivation of SARS-CoV-2 for Downstream Biological Assays. *J. Infect. Dis.* **2020**, *222*, 1462–1467, doi:10.1093/infdis/jiaa507.
24. Wang, T.T.; Lien, C.Z.; Liu, S.; Selvaraj, P. Effective Heat Inactivation of SARS-CoV-2. *medRxiv* **2020**, 2020.04.29.20085498, doi:10.1101/2020.04.29.20085498.
25. Ratnesar-Shumate, S.; Williams, G.; Green, B.; Krause, M.; Holland, B.; Wood, S.; Bohannon, J.; Boydston, J.; Freeburger, D.; Hooper, I.; et al. Simulated Sunlight Rapidly Inactivates SARS-CoV-2 on Surfaces. *J. Infect. Dis.* **2020**, *222*, 214–222, doi:10.1093/infdis/jiaa274.
26. Kratzel, A.; Todt, D.; V'kovski, P.; Steiner, S.; Gultom, M.; Thao, T.T.N.; Ebert, N.; Holwerda, M.; Steinmann, J.; Niemeyer, D.; et al. Inactivation of Severe Acute Respiratory Syndrome Coronavirus 2 by WHO-Recommended Hand Rub Formulations and Alcohols - Volume 26, Number 7—July 2020 - Emerging Infectious Diseases Journal - CDC., doi:10.3201/eid2607.200915.
27. Meyers, C.; Kass, R.; Goldenberg, D.; Milici, J.; Alam, S.; Robison, R. Ethanol and Isopropanol Inactivation of Human Coronavirus on Hard Surfaces. *J. Hosp. Infect.* **2021**, *107*, 45–49, doi:10.1016/j.jhin.2020.09.026.
28. Pascoe, M.J.; Robertson, A.; Crayford, A.; Durand, E.; Steer, J.; Castelli, A.; Wesgate, R.; Evans, S.L.; Porch, A.; Maillard, J.-Y. Dry Heat and Microwave-Generated Steam Protocols for the Rapid Decontamination of Respiratory Personal Protective Equipment in Response to COVID-19-Related Shortages. *J. Hosp. Infect.* **2020**, *106*, 10–19, doi:10.1016/j.jhin.2020.07.008.
29. Inagaki, H.; Saito, A.; Sudaryatma, P.E.; Sugiyama, H.; Okabayashi, T.; Fujimoto, S. Rapid Inactivation of SARS-CoV-2 with Ozone Water. *bioRxiv* **2020**, 2020.11.01.361766, doi:10.1101/2020.11.01.361766.
30. Saini, V.; Sikri, K.; Batra, S.D.; Kalra, P.; Gautam, K. Development of a Highly Effective Low-Cost Vaporized Hydrogen Peroxide-Based Method for Disinfection of Personal Protective

Equipment for Their Selective Reuse during Pandemics. *Gut Pathog.* **2020**, *12*, doi:10.1186/s13099-020-00367-4.

31. Solar Ultraviolet Radiation Sensitivity of SARS-CoV-2 - The Lancet Microbe Available online: https://www.thelancet.com/journals/lanmic/article/PIIS2666-5247(20)30013-6/fulltext (accessed on 19 January 2021).
32. Heilingloh, C.S.; Aufderhorst, U.W.; Schipper, L.; Dittmer, U.; Witzke, O.; Yang, D.; Zheng, X.; Sutter, K.; Trilling, M.; Alt, M.; et al. Susceptibility of SARS-CoV-2 to UV Irradiation. *Am. J. Infect. Control* **2020**, *48*, 1273–1275, doi:10.1016/j.ajic.2020.07.031.
33. Viscusi, D.J.; Bergman, M.S.; Eimer, B.C.; Shaffer, R.E. Evaluation of Five Decontamination Methods for Filtering Facepiece Respirators. *Ann. Occup. Hyg.* **2009**, *53*, 815–827, doi:10.1093/annhyg/mep070.
34. Siddharta, A.; Pfaender, S.; Vielle, N.J.; Dijkman, R.; Friesland, M.; Becker, B.; Yang, J.; Engelmann, M.; Todt, D.; Windisch, M.P.; et al. Virucidal Activity of World Health Organization–Recommended Formulations Against Enveloped Viruses, Including Zika, Ebola, and Emerging Coronaviruses. *J. Infect. Dis.* **2017**, *215*, 902–906, doi:10.1093/infdis/jix046.
35. Chou, R.; Dana, T.; Buckley, D.I.; Selph, S.; Fu, R.; Totten, A.M. Epidemiology of and Risk Factors for Coronavirus Infection in Health Care Workers: A Living Rapid Review. *Ann. Intern. Med.* **2020**, *173*, 120–136, doi:10.7326/M20-1632.
36. Phua, J.; Weng, L.; Ling, L.; Egi, M.; Lim, C.-M.; Divatia, J.V.; Shrestha, B.R.; Arabi, Y.M.; Ng, J.; Gomersall, C.D.; et al. Intensive Care Management of Coronavirus Disease 2019 (COVID-19): Challenges and Recommendations. *Lancet Respir. Med.* **2020**, *8*, 506–517, doi:10.1016/S2213-2600(20)30161-2.
37. de Perio, M.A.; Dowell, C.H.; Delaney, L.J.; Radonovich, L.J.; Kuhar, D.T.; Gupta, N.; Patel, A.; Pillai, S.K.; D'Alessandro, M. Strategies for Optimizing the Supply of N95 Filtering Facepiece Respirators During the Coronavirus Disease 2019 (COVID-19) Pandemic. *Disaster Med. Public Health Prep.* 1–12, doi:10.1017/dmp.2020.160.
38. Strategies for Optimizing the Supply of N95 Respirators: COVID-19 | CDC Available online: https://www.cdc.gov/coronavirus/2019-ncov/hcp/respirators-strategy/index.html (accessed on 31 January 2021).
39. CDC Healthcare Workers Available online: https://www.cdc.gov/coronavirus/2019-ncov/hcp/respirators-strategy/index.html (accessed on 31 January 2021).
40. Mills, D.; Harnish, D.A.; Lawrence, C.; Sandoval-Powers, M.; Heimbuch, B.K. Ultraviolet Germicidal Irradiation of Influenza-Contaminated N95 Filtering Facepiece Respirators. *Am. J. Infect. Control* **2018**, *46*, e49–e55, doi:10.1016/j.ajic.2018.02.018.
41. Heimbuch, B.K.; Wallace, W.H.; Kinney, K.; Lumley, A.E.; Wu, C.-Y.; Woo, M.-H.; Wander, J.D. A Pandemic Influenza Preparedness Study: Use of Energetic Methods to Decontaminate Filtering Facepiece Respirators Contaminated with H1N1 Aerosols and Droplets. *Am. J. Infect. Control* **2011**, *39*, e1-9, doi:10.1016/j.ajic.2010.07.004.
42. Lore, M.B.; Heimbuch, B.K.; Brown, T.L.; Wander, J.D.; Hinrichs, S.H. Effectiveness of Three Decontamination Treatments against Influenza Virus Applied to Filtering Facepiece Respirators. *Ann. Occup. Hyg.* **2012**, *56*, 92–101, doi:10.1093/annhyg/mer054.
43. Evaluation of Multiple (3-Cycle) Decontamination Processing for Filtering Facepiece Respirators - Michael S. Bergman, Dennis J. Viscusi, Brian K. Heimbuch, Joseph D. Wander,

Anthony R. Sambol, Ronald E. Shaffer, 2010 Available online: https://journals.sagepub.com/doi/abs/10.1177/155892501000500405 (accessed on 19 January 2021).

44. Seresirikachorn, K.; Phoophiboon, V.; Chobarporn, T.; Tiankanon, K.; Aeumjaturapat, S.; Chusakul, S.; Snidvongs, K. Decontamination and Reuse of Surgical Masks and N95 Filtering Facepiece Respirators during the COVID-19 Pandemic: A Systematic Review. *Infect. Control Hosp. Epidemiol.* **2021**, *42*, 25–30, doi:10.1017/ice.2020.379.
45. Hydrogen Peroxide Vapor Sterilization of N95 Respirators for Reuse | MedRxiv Available online: https://www.medrxiv.org/content/10.1101/2020.03.24.20041087v1 (accessed on 19 January 2021).
46. Commissioner, O. of the Investigating Decontamination and Reuse of Respirators in Public Health Emergencies. *FDA* **2020**.
47. Dennis, R.; Pourdeyhimi, B.; Cashion, A.; Emanuel, S.; Hubbard, D. Durability of Disposable N95 Mask Material When Exposed to Improvised Ozone Gas Disinfection. *J. Sci. Med.* **2020**, *2*, doi:10.37714/josam.v2i1.37.
48. Ran, L.; Chen, X.; Wang, Y.; Wu, W.; Zhang, L.; Tan, X. Risk Factors of Healthcare Workers With Coronavirus Disease 2019: A Retrospective Cohort Study in a Designated Hospital of Wuhan in China. *Clin. Infect. Dis.* **2020**, *71*, 2218–2221, doi:10.1093/cid/ciaa287.
49. Human Coronavirus OC43 - an Overview | ScienceDirect Topics Available online: https://www.sciencedirect.com/topics/veterinary-science-and-veterinary-medicine/human-coronavirus-oc43 (accessed on 19 January 2021).
50. Zhu, Z.; Lian, X.; Su, X.; Wu, W.; Marraro, G.A.; Zeng, Y. From SARS and MERS to COVID-19: A Brief Summary and Comparison of Severe Acute Respiratory Infections Caused by Three Highly Pathogenic Human Coronaviruses. *Respir. Res.* **2020**, *21*, 224, doi:10.1186/s12931-020-01479-w.
51. KHAZAIELI, A.; Rowe, A. Vacuum-Based Method and Apparatus for Cleaning Soiled Articles 2019.
52. Llanes, A.; Restrepo, C.M.; Caballero, Z.; Rajeev, S.; Kennedy, M.A.; Lleonart, R. Betacoronavirus Genomes: How Genomic Information Has Been Used to Deal with Past Outbreaks and the COVID-19 Pandemic. *Int. J. Mol. Sci.* **2020**, *21*, doi:10.3390/ijms21124546.
53. Zamorano Cuervo, N.; Grandvaux, N. ACE2: Evidence of Role as Entry Receptor for SARS-CoV-2 and Implications in Comorbidities. *eLife* **2020**, *9*, e61390, doi:10.7554/eLife.61390.
54. Wijdicks, E.F.M. Historical Lessons from Twentieth-Century Pandemics Due to Respiratory Viruses. *Neurocrit. Care* **2020**, 1–6, doi:10.1007/s12028-020-00983-7.
55. Morens, D.M.; Daszak, P.; Taubenberger, J.K. Escaping Pandora's Box — Another Novel Coronavirus. *N. Engl. J. Med.* **2020**, *382*, 1293–1295, doi:10.1056/NEJMp2002106.
56. Transmission of SARS-CoV-2: Implications for Infection Prevention Precautions Available online: https://www.who.int/news-room/commentaries/detail/transmission-of-sars-cov-2-implications-for-infection-prevention-precautions (accessed on 19 January 2021).
57. Elvis, A.M.; Ekta, J.S. Ozone Therapy: A Clinical Review. *J. Nat. Sci. Biol. Med.* **2011**, *2*, 66–70, doi:10.4103/0976-9668.82319.

58. Photodissociation - an Overview | ScienceDirect Topics Available online: https://www.sciencedirect.com/topics/earth-and-planetary-sciences/photodissociation (accessed on 19 January 2021).
59. Kim, C.K.; Gentile, D.M.; Sproul, O.J. Mechanism of Ozone Inactivation of Bacteriophage F2. *Appl. Environ. Microbiol.* **1980**, *39*, 210–218, doi:10.1128/AEM.39.1.210-218.1980.
60. Proceedings of the Pathological Society of Great Britain and Ireland. *J. Pathol. Bacteriol.* **1963**, *85*, 567–568, doi:10.1002/path.1700850242.
61. Roy, D.; Wong, P.K.; Engelbrecht, R.S.; Chian, E.S. Mechanism of Enteroviral Inactivation by Ozone. *Appl. Environ. Microbiol.* **1981**, *41*, 718–723, doi:10.1128/AEM.41.3.718-723.1981.
62. Sato, H.; Wananabe, Y.; Miyata, H. Virucidal Effect of Ozone Treatment of Laboratory Animal Viruses. *Exp. Anim.* **1990**, *39*, 223–229, doi:10.1538/expanim1978.39.2_223.
63. Inactivation of Surface Viruses by Gaseous Ozone - PubMed Available online: https://pubmed.ncbi.nlm.nih.gov/18561570/ (accessed on 19 January 2021).
64. Hudson, J.B.; Sharma, M.; Petric, M. Inactivation of Norovirus by Ozone Gas in Conditions Relevant to Healthcare. *J. Hosp. Infect.* **2007**, *66*, 40–45, doi:10.1016/j.jhin.2006.12.021.
65. Dubuis, M.-E.; Dumont-Leblond, N.; Laliberté, C.; Veillette, M.; Turgeon, N.; Jean, J.; Duchaine, C. Ozone Efficacy for the Control of Airborne Viruses: Bacteriophage and Norovirus Models. *PLOS ONE* **2020**, *15*, e0231164, doi:10.1371/journal.pone.0231164.
66. Arkhipov, S. Antiviral and antibacterial effects of ozone. In; 2020; pp. 5–14.
67. EXAMINATION OF THE EFFICACY OF OZONE SOLUTION DISINFECTANT IN IN ACTIVATING SARS VIRUS--《Chinese Journal of Disinfection》2004 年 01 期 Available online: https://en.cnki.com.cn/Article_en/CJFDTotal-ZGXD200401010.htm (accessed on 19 January 2021).
68. Fontes, B.; Cattani Heimbecker, A.M.; de Souza Brito, G.; Costa, S.F.; van der Heijden, I.M.; Levin, A.S.; Rasslan, S. Effect of Low-Dose Gaseous Ozone on Pathogenic Bacteria. *BMC Infect. Dis.* **2012**, *12*, 358, doi:10.1186/1471-2334-12-358.
69. Full Article: Ozone: A Potential Oxidant for COVID-19 Virus (SARS-CoV-2) Available online: https://www.tandfonline.com/doi/full/10.1080/01919512.2020.1795614 (accessed on 19 January 2021).
70. Virion Disruption by Ozone-Mediated Reactive Oxygen Species - PubMed Available online: https://pubmed.ncbi.nlm.nih.gov/18598719/ (accessed on 19 January 2021).
71. Environmental and Decontamination Issues for Human Coronaviruses and Their Potential Surrogates - Cimolai - 2020 - Journal of Medical Virology - Wiley Online Library Available online: https://onlinelibrary.wiley.com/doi/10.1002/jmv.26170 (accessed on 19 January 2021).
72. Full Article: Development of a Practical Method for Using Ozone Gas as a Virus Decontaminating Agent Available online: https://www.tandfonline.com/doi/full/10.1080/01919510902747969 (accessed on 19 January 2021).